Journal of Electron Devices, Vol. 19, 2014, pp. 1654-1662

© JED [ISSN: 1682 -3427]

Journal of Electron Devices
www.jeldev.org

ANALYTICAL COMPUTATION OF DENSITY OF STATES OF ONE-DIMENSIONAL PHOTONIC CRYSTAL UNDER POLARIZED INCIDENT WAVE FOR DIFFERENT MATERIALS

Sourangsu Banerji, Abhishek Halder, Arpan Deyasi, Sayan Bose, Subhasis Mandal
Department of Electronics & Communication Engineering
RCC Institute of Information Technology
Canal South Road, Beliaghata, Kolkata-700015
sourangsu.banerji@gmail.com

Received 23-03-2014, online 3-04-2014

ABSTRACT

In this paper, a comparative analysis is made for density of states function of one-dimensional finite photonic crystal for both s and p-polarized wave incidences with different material compositions. Computation is carried out for $Al_xGa_{1-x}N/GaN$ heterostructure, and results are compared with conventional SiO_2/Air composition. Structural parameters of the periodic arrangement are suitably varied to observe the effect on the density of states, and observations are graphically represented by blueshift and redshift. For the $Al_xGa_{1-x}N/GaN$ material composition, Adachi's model has been considered to incorporate the dependencies of refractive indices on operative wavelength and material composition. Occurrence of the peak positions in both the cases speaks about the possible emission/detection wavelength range and shows the superiority of the semiconductor heterostructure based composition in fabricating a photonic crystal based optical transmitter/receiver.

Keywords: One-dimensional photonic crystal, Density of states, Polarized wave incidence, Semiconductor heterostructure, Blueshift and Redshift

I. INTRODUCTION

One-dimensional photonic crystal is an arrangement of materials with special periodicity in dielectric constant along the direction of propagation of electromagnetic wave [1]. Because of this periodicity, the structure exhibits a few windows in otherwise prohibited wavelength spectra, making it usable as a tunable optical bandpass filter [2-3] for photonic integrated circuit applications. This is possible due to the formation of photonic bandgap [4], which may be exhibited in one, two or three dimensions. This is a revolutionary building block for the future optical communication, and can be used in photonic integrated circuits [5]. These structures are capable of operating in the microwave, millimeter-wave, infrared and visible ranges of electromagnetic spectra, and are already used to fabricate various optical devices [6-9]. Among the different structures, one-dimensional periodic arrangement is most studied due to the inherent advantage of theoretically analyzing the optical characteristics for various applications. Theoretical investigations are also well supported by experimental workers due to the rapid advancement in microelectronics field.

Density of states of a photonic crystal has the importance for calculating

emission and absorption properties of molecules when they are placed inside the cavities of crystal [10]. Tuning of these properties are very important for fabrication of micro-laser or optical memory. Also threshold voltage of a laser may be reduced by modifying the DOS profile. Hence the accurate evaluation of density of states and its dependence on structural play a very important role when the structure is subjected to polarized incident wave as well as different material composition.

Rudzinski [11] calculated the density of states of a defected photonic crystal by analytical method. On similar lines, Kano [12] calculated DOS for anisotropic 3D photonic crystal for thermally pumped terahertz emission. Boundary effects on DOS are computed in [13] using Green's function. Dispersion relation of an N-period crystal was theoretically investigated by Dios-Leyva [14] and compared with the result of an infinite one for finite and large values of unit cells. Mode spectrum is also calculated in [11], [14] for 1D structure by several workers. Scotognella [15] suggested that 1D PC with suitable material composition can be used as DFB laser.

In this paper, density of states of one-dimensional photonic crystal is analytically computed as a function of normalized wavelength under different polarized incident wave conditions for different material composition. SiO_2/Air, which is an industry standard today in fabricating photonic crystals is taken as one of the material composition and $Al_xGa_{1-x}N$/GaN, a semiconductor heterostructure is taken as another. Use of $Al_xGa_{1-x}N$/GaN material composition has been taken up because as shown in [16] that the effect of carrier localization in $Al_xGa_{1-x}N$ layer is expected to increase the overall figure of merit of the $Al_xGa_{1-x}N$/GaN due to the combined advantages of enhanced band offset, lattice mismatch induced piezoelectric effect. Thus improving the material quality of AlGaN alloys is also of crucial importance for fabricating high performance $Al_xGa_{1-x}N$/GaN structures. The advantages of GaN can be summarized as ruggedness, power handling and low loss [17], [18]. Authors already calculated the DOS for heterostructure only [19], but comparison with conventional materials are not published as far the knowledge of the authors. S and P type polarizations are considered for comparative analysis and variation of periodic layer dimensions are incorporated to observe the effect on DOS. Results are important for photonic crystal based optical emitter/ detector applications**.**

II. MATHEMATICAL MODELING

Using the periodic boundary condition, let us consider that the k-space volume occupied by each wave vector point $\frac{V}{(2\pi)^3}$ is derived by discretizing the wave vector and taking the quantization volume V to infinity. The number of modes, δN having frequencies from ω to dω is given by,

$$\delta N = \rho(\omega)\delta\omega = \left[\frac{V}{(2\pi)^3}\right]\sum_n \int_{all,k(\omega_n)} d^3k = \left[\frac{V}{(2\pi)^3}\right]\sum_n \int_{all,k(\omega_n)} dk_n dS_n \quad (1)$$

where dS_n and dk_n represent the infinitesimally small area and thickness of the surface elements on a constant-frequency surface in k space and band index is given by n.

So, making use of the approximations,

$$\left(\frac{\partial \omega_{nk}}{\partial k_n}\right)\partial k_n = \delta\omega \tag{2}$$

$$\left|\nabla_k \omega_{nk}\right| = \frac{\partial \omega_{nk}}{\partial k_n} \tag{3}$$

and taking $\delta\omega \to 0$ we get,

$$\rho(\omega) = \left[\frac{V}{(2\pi)^3}\right]\sum_n \int_{all,k(\omega_n)} \frac{dS_n}{\left|\nabla_k \omega_{nk}\right|} \ . \tag{4}$$

Now if we confine the Bloch waves in 1D, i.e., the ones normal to the superlattice, the only possible wave vectors corresponding to each ω are $+k_B$ and -. k_B .

Then we can write Eqn. (1) as,

$$\begin{aligned}\delta N &= \left[\frac{L}{2\pi}\right]\sum_n \int_{all,k(\omega_n)} dk_B \\ &= \sum_n \int_{all,k(\omega_n)} \left(\frac{\partial k_B}{\partial \omega}\right)\delta\omega\end{aligned} \tag{5}$$

where

$$\rho(\omega) = \left[\frac{L}{\pi}\right]\frac{\partial k_B}{\partial \omega} \ . \tag{6}$$

Now, in the 1D periodic structure the wave vector in the superlattice is $k = (k_B, k_y, k_z)$ where k_B is the Bloch wave component and

$$\beta = \sqrt{{k_y}^2 + {k_z}^2} \tag{7}$$

is the conserved tangential wave number.

Now, considering dependence of propagation vectors k_{1x} and k_{2x} on refractive indices in different media as,

$$k_{(1,2)x} = \frac{\omega}{c}\sqrt{{n_{(1,2)}}^2 - n^2} \tag{8}$$

and,

$$k_{(1,2)x} d_{(1,2)} = 2\pi \frac{d_{(1,2)}}{L}\frac{L}{\lambda}\sqrt{{n_{(1,2)}}^2 - n^2} \tag{9}$$

we may write for S-polarized wave

$$\begin{aligned}\cos(K_B L) &= \cos(k_{1x} d_1)\cos(k_{2x} d_2) \\ &-\frac{1}{2}\left(\frac{k_{1x}}{k_{2x}} + \frac{k_{2x}}{k_{1x}}\right)\sin(k_{1x} d_1)\sin(k_{2x} d_2)\end{aligned} \tag{10}$$

and similarly, for P-polarization,

$$\begin{aligned}\cos(K_B L) &= \cos(k_{1x} d_1)\cos(k_{2x} d_2) \\ &-\frac{1}{2}\left(\frac{k_{1x}}{k_{2x}}\frac{n_2^2}{n_1^2} + \frac{k_{2x}}{k_{1x}}\frac{n_1^2}{n_2^2}\right)\sin(k_{1x} d_1)\sin(k_{2x} d_2)\end{aligned} \tag{11}$$

which can be written as

$$K_B = \frac{1}{L}\cos^{-1}\left[F(\omega,\beta)\right] \tag{12}$$

where

$$\begin{aligned}\left[F(\omega,\beta)\right] &= \cos(k_{1x} d_1)\cos(k_{2x} d_2) \\ &-\frac{1}{2}\left(\frac{k_{1x}}{k_{2x}}\frac{n_2^2}{n_1^2} + \frac{k_{2x}}{k_{1x}}\frac{n_1^2}{n_2^2}\right)\times \\ &\sin(k_{1x} d_1)\sin(k_{2x} d_2)\cdot\end{aligned} \tag{13}$$

Then for constant β

$$\left(\frac{\delta K_B}{\delta\omega}\right)_\beta = \frac{\left(-\frac{1}{L}\right)\left(\frac{\partial F}{\partial \omega}\right)\Big|_\beta}{\sqrt{1 - F^2(\omega,\beta)}} \ . \tag{14}$$

Thus the density of states reads

$$\rho(\omega) = \frac{V\omega^2}{4\pi^2 c^2}\int_0^{n_1}\left[\frac{n\left(-\frac{1}{L}\right)\left(\frac{\partial F}{\partial \omega}\right)\Big|_\beta}{\sqrt{1 - F^2(\omega,\beta)}}\right]dn \tag{15}$$

where $\rho_0(\omega)$ is the ideal density of states function.

From Eq. (15), we can write

$$\left(-\frac{1}{L}\right)\left(\frac{\partial F}{\partial \omega}\right)\Big|_n = \frac{1}{c}\frac{d_1}{L}\sqrt{n_1^{\,2}-n^2}\times$$
$$\left[\begin{array}{l}\sin(k_{1x}d_1)\cos(k_{2x}d_2)\\ +\frac{1}{2}\left(\frac{k_{1x}}{k_{2x}}+\frac{k_{2x}}{k_{1x}}\right)\times\\ \cos(k_{1x}d_1)\sin(k_{2x}d_2)\end{array}\right] \qquad (16)$$
$$+\frac{1}{c}\frac{d_2}{L}\sqrt{n_2^{\,2}-n^2}\times$$
$$\left[\begin{array}{l}\sin(k_{2x}d_2)\cos(k_{1x}d_1)\\ +\frac{1}{2}\left(\frac{k_{1x}}{k_{2x}}+\frac{k_{2x}}{k_{1x}}\right)\times\\ \cos(k_{2x}d_2)\sin(k_{1x}d_1)\end{array}\right]$$

This can be written in the following form

$$\left(-\frac{1}{L}\right)\left(\frac{n}{\omega}\right)\left(\frac{\partial F}{\partial \omega}\right)\Big|_n$$
$$=\frac{1}{c}\frac{d_1}{L}\frac{n^2}{\sqrt{n_1^{\,2}-n^2}}\times$$
$$\left[\begin{array}{l}\sin(k_{1x}d_1)\cos(k_{2x}d_2)+\\ \frac{1}{2}\left(\frac{k_{1x}}{k_{2x}}+\frac{k_{2x}}{k_{1x}}\right)\cos(k_{1x}d_1)\sin(k_{2x}d_2)\end{array}\right]$$
$$+\frac{1}{c}\frac{d_2}{L}\frac{n^2}{n_2^{\,2}-n^2}\times$$
$$\left[\begin{array}{l}\sin(k_{2x}d_2)\cos(k_{1x}d_1)+\\ \frac{1}{2}\left(\frac{k_{1x}}{k_{2x}}+\frac{k_{2x}}{k_{1x}}\right)\cos(k_{2x}d_2)\sin(k_{1x}d_1)\end{array}\right]$$
$$-\frac{1}{2L}\left(\frac{n}{\omega}\right)\frac{\partial}{\partial n}\left(\frac{k_{1x}}{k_{2x}}+\frac{k_{2x}}{k_{1x}}\right)\times$$
$$\sin(k_{1x}d_1)\sin(k_{2x}d_2)\cdot \qquad (17)$$

Similarly under p-polarization condition, the equation gets modified as

$$\left(-\frac{1}{L}\right)\left(\frac{n}{\omega}\right)\left(\frac{\partial F}{\partial \omega}\right)\Big|_n =$$
$$\frac{1}{c}\frac{d_1}{L}\frac{n^2}{\sqrt{n_1^{\,2}-n^2}}\times$$
$$\left[\begin{array}{l}\sin(k_{1x}d_1)\cos(k_{2x}d_2)+\\ \frac{1}{2}\left(\frac{n_2^2k_{1x}}{n_1^2k_{2x}}+\frac{n_1^2k_{2x}}{n_2^2k_{1x}}\right)\cos(k_{1x}d_1)\sin(k_{2x}d_2)\end{array}\right]$$
$$+\frac{1}{c}\frac{d_2}{L}\frac{n^2}{n_2^{\,2}-n^2}\times$$
$$\left[\begin{array}{l}\sin(k_{2x}d_2)\cos(k_{1x}d_1)+\\ \frac{1}{2}\left(\frac{n_2^2k_{1x}}{n_1^2k_{2x}}+\frac{n_1^2k_{2x}}{n_2^2k_{1x}}\right)\cos(k_{2x}d_2)\sin(k_{1x}d_1)\end{array}\right]$$
$$-\frac{1}{2L}\left(\frac{n}{\omega}\right)\frac{\partial}{\partial n}\left(\frac{n_2^2k_{1x}}{n_1^2k_{2x}}+\frac{n_1^2k_{2x}}{n_2^2k_{1x}}\right)\times$$
$$\sin(k_{1x}d_1)\sin(k_{2x}d_2)\cdot \qquad (18)$$

III. RESULTS AND DISCUSSION

The density of states function of one-dimensional infinite photonic crystal have been computed for different dimensional configurations and also for different material compositions. Angular incidence of electromagnetic wave is considered for simulation which gives S or P' polarized wave due to formation of incomplete photonic bandgap. In fig. 1, density of states is plotted as a function of normalized wavelength for a constant mole fraction (x) of 0.15 for AlN in $Al_xGa_{1-x}N$ material composition for incidence of both the polarized light, whereas the dependence of SiO_2/Air on mole fraction is absent and thus a generalized plot for the latter composition.

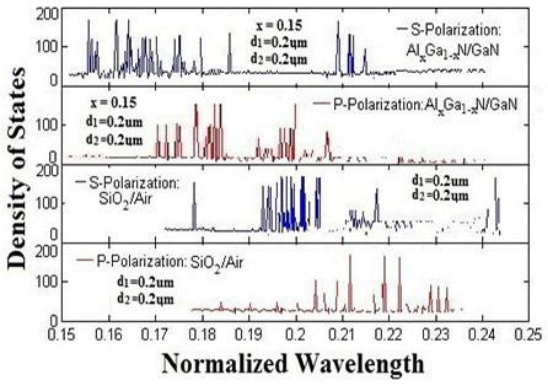

Figure 1: DOS with normalized wavelength for different material compositions

Here the layer thicknesses for both the compositions are matched. Redshift is observed for both the types of material composition and the magnitude of the shift in p-polarization is higher in both. However the magnitude of shift and the density of modes in much more in $Al_xGa_{1-x}N/GaN$ as compared to that in SiO_2/Air. Fig 2 shows the DOS profiles as a function of normalized wavelength for different thicknesses of lower refractive index material under s-polarized incident wave.

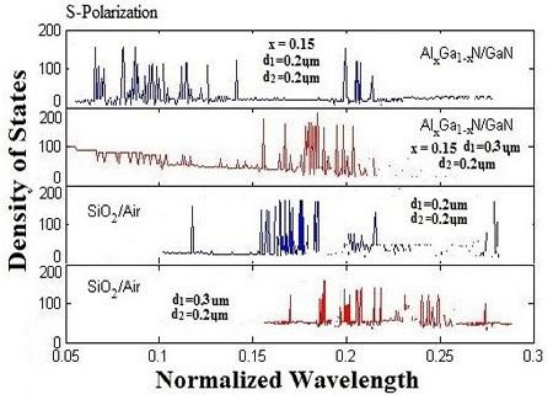

Figure 2a: DOS with normalized wavelength for increasing thicknesses of low refractive index material layer keeping dimension of high refractive index material layer constant (0.2 μm) for s-polarized wave

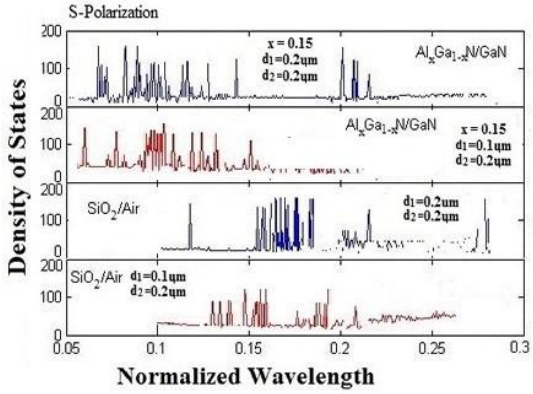

Figure 2b: DOS with normalized wavelength for decreasing thicknesses of low refractive index material layer keeping dimension of high refractive index material layer constant (0.2 μm) for s-polarized wave

In the first two subplots of Fig. 2a, keeping the dimension of GaN layer (higher refractive index material) constant, thickness of $Al_xGa_{1-x}N$ is varied to observe the effect on density of states. In the last two subplots, now the dimension of SiO_2 layer is kept constant with the thickness of the Air layer being varied. A similar redshift is observed as the layer thickness increases in the case of lower refractive index material but the magnitude of peaks in case of SiO_2/Air is much less and scare as compared to $Al_xGa_{1-x}N/GaN$. In Fig. 2b, the first two subplots for $Al_xGa1_{-x}N/GaN$ material composition as well as the last two subplots for SiO_2/Air composition show blueshift. However, the magnitude of the peaks is more in case of SiO_2/Air than the former one i.e. $Al_xGa1_{-x}N/GaN$ with decreasing layer thickness.

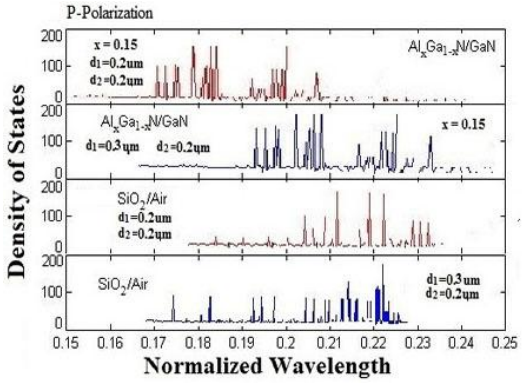

Figure 3a: DOS with normalized wavelength for increasing thicknesses of low refractive index material layer keeping dimension of high refractive index material layer constant (0.2 μm) for p-polarized wave

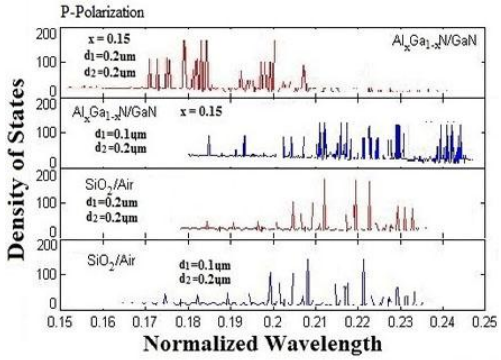

Figure 3b: Density of states with normalized wavelength for decreasing thicknesses of low refractive index material layer keeping dimension of high refractive index material layer constant (0.2 μm) for p-polarized wave

Fig 3 depicts the DOS profiles as a function of normalized wavelength for different thicknesses of lower refractive index material under p-polarized incident wave. Keeping the dimension of GaN layer constant, thickness of $Al_xGa_{1-x}N$ is varied. Similarly, the dimension of SiO_2 layer is kept constant with the thickness of the Air layer being varied to observe the effect on density of states. In Fig 3a, for $Al_xGa_{1-x}N$/GaN material composition a blueshift is observed with increasing layer thickness under the p-polarization condition with higher magnitude peaks. Contrary to this however we find that in case of SiO_2/Air composition, a redshift is observed with widely spread out peaks. However as seen in fig. 3b, we find out that in case of $Al_xGa_{1-x}N$/GaN the blueshift is more distinguishable and states are denser when the layer thickness is decreased contrary to the previous case where the blueshift was dominated with higher magnitude peaks for p-polarized light. In case of SiO_2/Air we get a relatively known DOS profile (if we closely follow the nature of the $Al_xGa_{1-x}N$/GaN case).Here with decreasing layer thickness, the redshift is relatively less than the former case and at points the DOS completely vanishes.

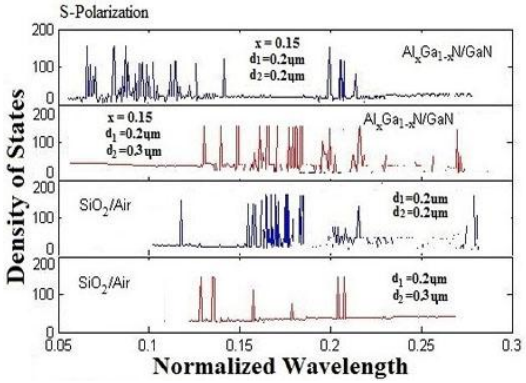

Figure 4a: Density of states with normalized wavelength for increasing thicknesses of high refractive index material layer keeping dimension of low refractive index material layer constant (0.2 μm) for s-polarized wave

Likewise, Fig. 4 shows the DOS profiles with normalized wavelength for different layer thicknesses under the incidence of s-polarized light. Here DOS function is plotted keeping dimension of lower refractive index layer constant, and varying the thickness of higher refractive index layer.

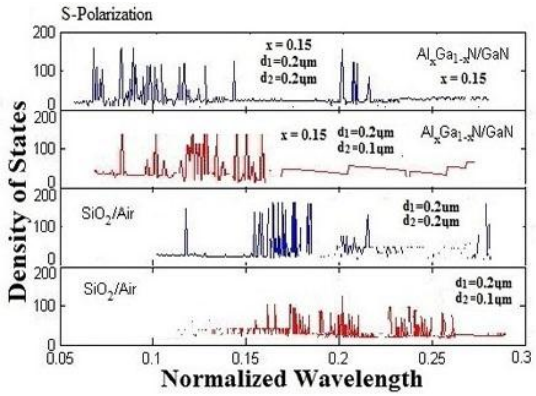

Figure 4b: Density of states with normalized wavelength for decreasing thicknesses of high refractive index material layer keeping dimension of low refractive index material layer constant (0.2 μm) for s-polarized wave

In Fig. 4a, the first two subplots depict that the $Al_xGa_{1-x}N$ layer (low refractive index) is fixed at 0.2 μm, while the GaN layer is varied with layer thickness for s-polarized wave incidence. The same thing is done with the last two subplots with the Air layer being constant this time with varying SiO_2 layer thickness.

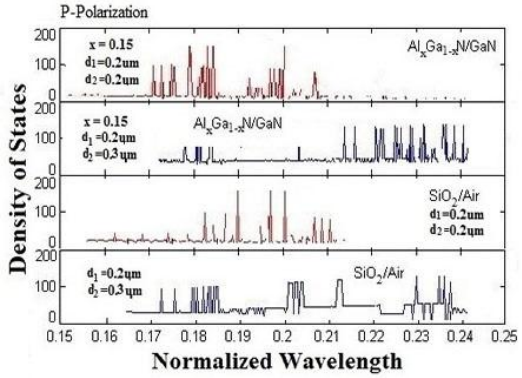

Figure 5a: Density of states with normalized wavelength for increasing thicknesses of high refractive index material layer keeping dimension of low refractive index material layer constant (0.2 μm) for p-polarized wave

For $Al_xGa_{1-x}N/GaN$ composition, prominent redshift is observed with increasing layer thickness with areas where the DOS completely disappears. Contrary to this in case of SiO_2/Air, blueshift is observed with higher value of peak magnitudes for s-polarized light. However, when the layer thickness of the higher refractive index decreases we find that redshift occurs for both the material compositions. But the peaks are more densely packed and higher in case of $Al_xGa_{1-x}N/GaN$ as compared to SiO_2/Air.

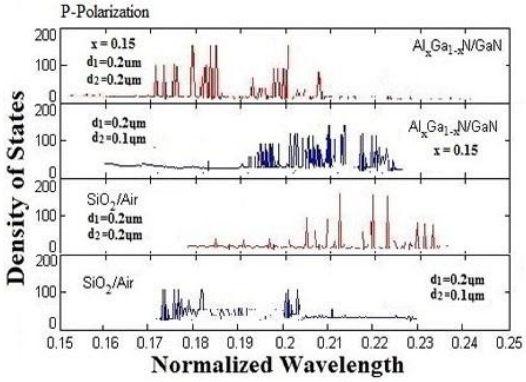

Figure 5b: Density of states with normalized wavelength for decreasing thicknesses of high refractive index material layer keeping dimension of low refractive index material layer constant (0.2 μm) for p-polarized wave

Fig. 5 shows the DOS profiles with normalized wavelength for different layer thicknesses under the incidence of p-polarized light, keeping the dimension of lower refractive index layer constant, and varying the thickness of higher refractive index layer. In Fig. 5a, prominent blueshift is observed for both the material compositions with increasing layer thickness. The magnitude of the peaks in case of $Al_xGa_{1-x}N/GaN$ composition is high and uniform. Fig. 5b is quite predictable in its nature. Here we see that for $Al_xGa_{1-x}N/GaN$ composition, blueshift is observed in contrast to which redshift is observed for SiO_2/Air material composition for decreasing layer thickness of the high refractive index material. One observable feature here is the distribution of the DOS profile for the SiO_2/Air. The DOS function nearly ceases to exist when the layer thickness of the high refractive index material is

reduced. A large number of spaces remain vacant.

IV. CONCLUSION

By suitably varying the structural parameters, density of states profiles of one-dimensional infinite photonic crystal have been studied in this paper. Comparative analysis is made between SiO_2/Air, the material composition widely used today in fabricating photonic emitter/detector with a potential candidate i.e. $Al_xGa_{1-x}N$/GaN. The advantages of this semiconductor heterostructure have already been discussed in the introductory part of this paper. Detailed mathematical formulations as well as simulations have provided us; with a complete picture regarding the operating range of the PC based devices fabricated using these material compositions, To sum up, we can say that from the study of the simulations in case of $Al_xGa_{1-x}N$/GaN composition, the operating range for the emitter/detector is increased compared to the conventional ones fabricated with SiO_2/Air. Moreover, the uniformity of the DOS profile in case of $Al_xGa_{1-x}N$/GaN composition guarantees us a hassle free operation in the operating range. The magnitude of the peaks and the predominance in either of the redshift or blueshift speaks for its stability of operation. One common reason for such advantages can be attributed to the fact that in case of semiconductor heterostructures we model the material composition in such a way so as to increase its contrast in refractive index.

References

[1] R. Loudon, "The Propagation of Electromagnetic Energy through an Absorbing Dielectric", Journal of Physics A, **3**, 233-245 (1970).

[2] D. Mao, Z. Ouyang, and J. C. Wang, "A Photonic-Crystal Polarizer Integrated with the Functions of Narrow Bandpass and Narrow Transmission Angle Filtering", Applied Physics B, **90**, 127-131 (2008).

[3] A. Maity, B. Chottopadhyay, U. Banerjee, and A. Deyasi, "Novel Band-pass Filter Design using Photonic Multiple Quantum Well Structure with P-polarized Incident Wave at 1550 nm", Journal of Electron Devices, **17**, 1400-1405 (2013).

[4] R. L. Wang, J. Zhang, and Q. F. Hu, "Simulation of Band Gap Structures of 1D Photonic Crystal", Journal of the Korean Physical Society, **52**, S71-S74, (2008).

[5] K. Bayat, G. Z. Rafi, G. S. A. Shaker, N. Ranjkesh, S. K. Chaudhuri, and S. Safavi-Naeini, "Photonic-Crystal based Polarization Converter for Terahertz Integrated Circuit", IEEE Transactions on Microwave Theory and Techniques, **58**, 1976-1984 (2010).

[6] P. Szczepański, "Semiclassical Theory of Multimode Operation of a Distributed Feedback Laser", IEEE Journal of Quantum Electronics, **24**, 1248-1257 (1988).

[7] J. C. Chen, H. A. Haus, S. Fan, P. R. Villeneuve, and J. D. Joannopoulos, "Optical Filters from Photonic Band Gap Air Bridges", Journal of Lightwave Technology, **14**, 2575-2580 (1996).

[8] I. S. Fogel, J. M. Bendickson, M. D. Tocci, M. J. Bloemer, M. Scalora, C. M. Bowden, and J. P. Dowling, "Spontaneous Emission and Nonlinear Effects in Photonic Bandgap Materials", Pure and Applied Optics: Journal of the European Optical Society Part A, **7**, 393-408 (1998).

[9] J. Hansryd, P. A. Andrekson, M. Westlund, J. Li, and P. O. Hedekvist, "Fiber-based Optical Parametric Amplifiers and their Applications," IEEE Journal of Selected Topics on Quantum Electronics, **8**, 506-520 (2002).

[10] T. Yamasaki, and T. Tsutsui, "Spontaneous Emission from Fluorescent Molecules Embedded in Photonic Crystals consisting of Polystyrene Microspheres", Applied Physics Letters, **72**, 1957-1959, (1998).

[11] A. Rudzinski, A. Tyszka-Zawadzka, and P. Szczepanski, "Simple Model of the Density of States in 1D Photonic Crystal", Proceedings of SPIE 2005, pp. 5950,-59501.

[12] P Kano, D Barker, M Brio, "Analysis of the Analytic Dispersion Relation and Density of States of A Selected Photonic Crystal", Journal of Physics D: Applied Physics, **41**, 185106, 2(008).

[13] V. Prosentsov, and A. Lagendijk, Periodicity Enclosed in Boundaries: "Local Density of States in Photonic Clusters", Optics Express, **16**, 6974-6984 (2008).

[14] M. de Dios-Leyva, and J. C. Drake-Pérez, "Properties of the Dispersion Relation in Finite One-dimensional Photonic Crystals", Journal of Applied Physics, **109**, 103526 (2011).

[15] F. Scotognella, A. Monguzzi, M. Cucini, F. Meinardi, D. Comoretto, and R. Tubino, "One Dimensional Polymeric Organic Photonic Crystals for DFB Lasers", International Journal of Photoenergy, 10.1155 389034, (2008).

[16] M. D. Hodge, R. Vetury and J. B. Shealy, "Fundamental failure mechanisms limiting maximum voltage operation in AlGaN/GaN HEMTs", Reliability Physics Symposium (IRPS), 2012 IEEE International, IEEE, (2012).

[17] M. Hadis, "Handbook of Nitride Semiconductors and Devices", GaN-based Optical and Electronic Devices, Wiley (2009).

[18] P. C. Hoang, "Applications of Photonic Crystals in Communications Engineering and Optical Imaging", Diss. Universitätsbibliothek, (2009).

[19] S. Banerji, A. Deyasi, A. Halder, and S. Bose, "Comparative Study of Density of States of 1D Photonic Crystal for Different Polarization Conditions of Incident Wave", International Conference on Electronics, Communication and Instrumentation [ICECI: 14], pp. 1-4, Jan 2014 doi: 10.1109/ICECI.2014.6767359 .